Practical implementation of a Novel Temperature-Insensitive Aging Indicator for on-line monitoring of bond-wire degradation in IGBT power modules

Zoubir Khatir, Ali Ibrahim, Richard Lallemand

Practical implementation of a Novel Temperature-Insensitive Aging Indicator for on-line monitoring of bond-wire degradation in IGBT power modules

Zoubir Khatir, SATIE, Univ. Eiffel, Versailles, France, zoubir.khatir@univ-eiffel.fr
Ali Ibrahim, SATIE, Univ. Eiffel, Versailles, France, ali.ibrahim@univ-eiffel.fr
Richard Lallemand, SATIE, Univ. Eiffel, Versailles, France, richard.lallemand@univ-eiffel.fr

Keywords

Health assessment, Diagnostics, Zero temperature coefficient, Condition monitoring, Aging indicator.

Abstract

The online assessment of the health status of power electronic modules is crucial for predictive maintenance, enabling better system reliability and optimized operational efficiency. Traditional aging indicators are often impractical for online monitoring due to their complexity and high implementation costs, particularly because they require junction temperature estimation. In this paper, we focus on the practical implementation of a novel, temperature-insensitive aging indicator tailored for on-line monitoring bond-wire degradation in IGBT power modules. This method, based on the analysis of zero-temperature coefficient (ZTC) of I-V characteristics with degraded top-metal interconnects, allows for an efficient and cost-effective monitoring solution. It is presented an experimental validation through power cycling tests, highlighting the feasibility of real-time application. The proposed indicator shows a strong correlation with conventional aging indicators while offering enhanced sensitivity and independence from temperature variations. Furthermore, we outline a robust methodology for integrating this approach into industrial or embedded applications, ensuring scalability and ease of deployment.

Introduction

The reliability of power electronic systems is a key research area, especially in applications requiring high availability and long operational lifetimes. Condition Monitoring (CM) techniques are widely used for health assessment, yet their implementation in real-time industrial environments remains a challenge due to the difficulty of measuring junction temperature in field conditions. Several review papers have addressed CM issues and challenges [1,2]. The main damage mechanisms for IGBT power modules during power cycles typically involve bond wire connections and solder layers. Conventional indicators include on-state voltage for detecting bond-wire degradations, as well as thermal resistance and junction temperature measurements. These indicators are easily observed in laboratory but are difficult to apply in online operations. Specifically, measuring Vce for top-side interconnection degradations in IGBTs is challenging and needs junction temperature measurement.

Recent research has explored alternative aging indicators, particularly those that do not depend on temperature. The Zero-Temperature Coefficient (ZTC) point of the forward I-V characteristics of bipolar devices has shown promise for aging detection (fig.1).

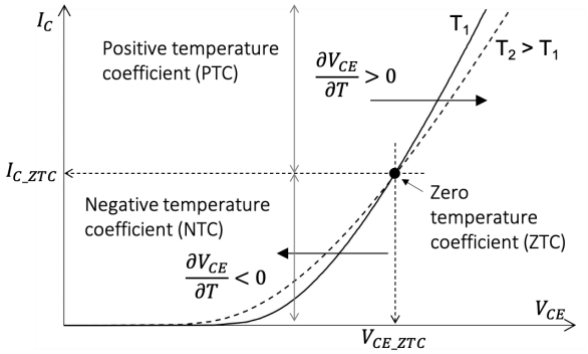

Fig.1: IGBT schematic I-V characteristics for two temperature levels T1 and T2 (T2 > T1).

This point separates two zones in the I-V characteristics: the positive temperature coefficient (PTC) zone for current levels $I_C > I_{C\_ZTC}$ and the negative temperature coefficient (NTC) zone for current levels $I_C < I_{C\_ZTC}$.

Authors in [5] and [6] propose a method for monitoring bond-wire degradations in IGBT modules based on the ZTC point by measuring V_{CE} at the I_{C_ZTC} current value. They hypothesize that the current I_{C_ZTC} is independent of the state of health while V_{CE_ZTC} increases with aging, but this hypothesis is not demonstrated. In [7], authors investigated the influence of different degradation mechanisms and observed effects similar to bond-wire lift-off but could not demonstrate result repeatability. They assumed that the ZTC could be used for monitoring with minor current modifications, focusing on V_{CE} variations due to degradation. However, previous studies have mistakenly expected significant impacts on V_{CE_ZTC} with negligible effects on I_{C_ZTC}.

In a previous paper [8], a new aging parameter has been theoretically presented with some experimental results for validation. The present document is an extension of the latter, focusing on practical implementation with a full experimental demonstration.

Initial experimental observations

The tested devices were chosen in such a way that only damages at bond-wire contacts take place during aging. These ones (figs.2 and 3) are commercial devices and have been referred to as "device A" and "device B" in the following.

Fig. 2 shows the measured on-state characteristics of the high side switch of the device A, at 20°C and 100°C and for both a fresh and aged devices. During aging tests, the saturation V_{CE} voltage, which is a classical aging indicator, has also been measured at high current (100A) and at a known temperature (55°C). Using this "classical" aging indicator, the degraded device characteristics in fig.2 corresponds to an increase of 5% in V_{CE}.

It can be seen the ZCT point evolution from the healthy state (ZCTh) to the degraded state (ZCTd). Moreover, one can observe that ZCTd point is as well defined as the ZCTh point and is located at a clearly lower current level and very slightly shifted to the left. The table gives the results of the measured values for high and low sides switches. For the high side, the current level of the ZTC point has decreased of about 23% (8.5A) and the saturation voltage has decreased of about 1.7% (20mV). The same tendencies were observed for the low side where the corresponding variations are 6.06 A (15%) and 22mV (1.9%).

Similarly, fig.3 shows the measured I-V characteristics of the high side switch of device B. As the switch is composed of 4 paralleled chips, the ZTC current levels are much higher.

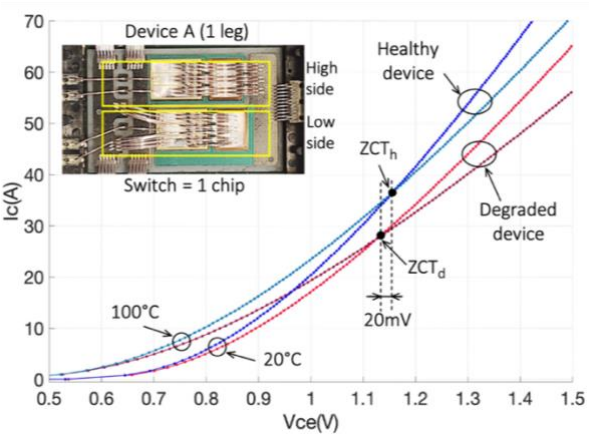

High Side				Low Side			
I_{ZCTh} (A)	I_{ZCTd} (A)	V_{ZCTh} (V)	V_{ZCTd} (V)	I_{ZCTh} (A)	I_{ZCTd} (A)	V_{ZCTh} (V)	V_{ZCTd} (V)
36.50	28.00	1.154	1.134	41.06	35.00	1.143	1.121
ΔI_{ZCT}		ΔV_{ZCT}		ΔI_{ZCT}		ΔV_{ZCT}	
8.5 A (23%)		20 mV (1.7%)		6.06 A (15%)		22 mV (1.9%)	

Fig.2 Measured on-characteristics of high-side switch "device A" for healthy and aged devices.

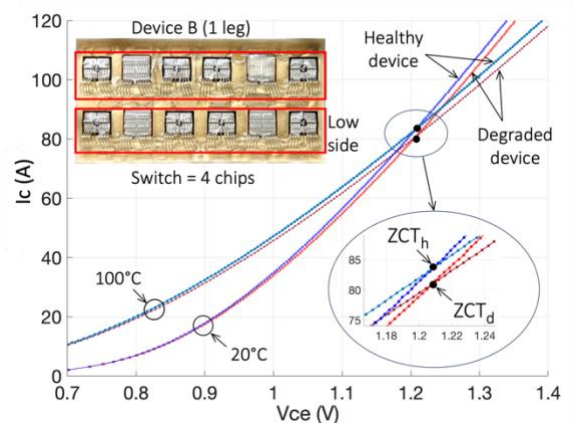

High Side				Low Side			
I_{ZCTh} (A)	I_{ZCTd} (A)	V_{ZCTh} (V)	V_{ZCTd} (V)	I_{ZCTh} (A)	I_{ZCTd} (A)	V_{ZCTh} (V)	V_{ZCTd} (V)
83.9	80.9	1.209	1.208	84.3	80.6	1.210	1.205
ΔI_{ZCT}		ΔV_{ZCT}		ΔI_{ZCT}		ΔV_{ZCT}	
3.0 A (3.7%)		1 mV (0.1%)		3.7 A (4.4%)		5 mV (0.4%)	

Fig.3 Measured on-characteristics of high-side switch "device B" for healthy and aged devices.

In this case, throughout the aging test, the classical V_{CE} indicator is regularly measured at 100A and at 55°C. Using this conventional aging indicator, the degraded device exhibits here an increase of 2% in V_{CE}. Figure 3 gives the results of the measured values for both switches of device B. For the high side switch, the I_{C_ZTC} has decreased of about 3.7% (3A) and the V_{CE_ZTC} has

decreased of about 0.1% (1 mV) whereas the corresponding values for the low side are 3.7 A (4.4%) and 5 mV (0.4%).

In summary, the results obtained show that the qualitative evolution of the ZTC point with aging remains similar whether the switches are single-chip or multiple-chip in parallel. It has been observed a significant drop in I_{C_ZTC} level and a very small drop in V_{CE_ZTC}.

Practical implementation

Implementation Protocol

The proposed method is implemented in two main steps. It consists first in determining, during operation, the ZTC point. This involves identifying the characteristic voltage V_{CE_ZTC}, which remains nearly constant, and the corresponding collector current I_{C_ZTC0}, which serves as the initial (or reference) value of the aging indicator. Then, in a second step, monitor the value of the I_{C_ZTC} which will give us the state of aging of the power module. Both steps are performed in real-time and online without requiring additional offline measurements.

Step 1 : determination of the ZTC point (identification of the characteristic voltage V_{CE_ZTC}, and reference value I_{C_ZTC0})

This step involves measuring simultaneously the collector current I_C and the collector-emitter voltage V_{CE} while these quantities vary during operation, during a short period. The objective is to identify the voltage V_{CE_ZTC}, initially estimated from the device datasheet, and determine the corresponding initial reference current I_{C_ZTC0}.

To achieve this, V_{CE} and I_C must be recorded with sufficient sampling resolution in a window around the expected V_{CE_ZTC} value. This process should be conducted twice at the beginning of the power module's operational life, under two different thermal conditions – one at a lower temperature (e.g., cold start) and the other at a higher temperature (e.g., after warm-up). There is no need to know the temperature values; it is sufficient that the two conditions correspond to distinct thermal states.

This step leads to draw the measured I-V characteristics at two unknown but different temperatures and to determine experimentally on-line the ZCT point, i.e. the characteristic value V_{CE_ZTC}, and the initial value I_{C_ZTC0}.

Step 2 : Monitoring the aging indicator (I_{C_ZTC})

Once the initial ZTC point has been determined, the next step involves continuously monitoring the aging indicator I_{C_ZTC} during operation.

- The monitoring process follows the same principle as the first step: whenever V_{CE} crosses the predetermined V_{CE_ZTC} value, both voltage and collector current are recorded in a small observation window around this point (see Fig. 4).
- If the data sampling rate is insufficient to capture the value of I_{C_ZTC}, interpolation techniques (as illustrated in Fig. 4) can be applied to refine the measurement.

By tracking the evolution of I_{C_ZTC} over time, degradation of the power module can be assessed, providing an online diagnostic tool for aging and reliability evaluation.

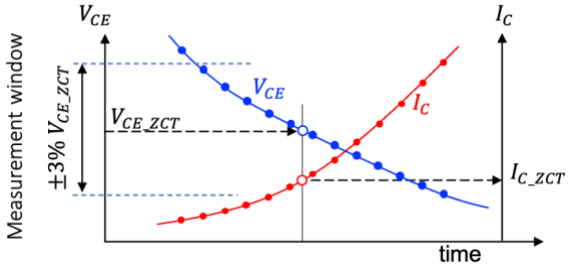

Fig.4 Measurement principle of the I_{C_ZTC}.

Which sensitivity to temperature and to correct V_{CE_ZTC} characteristic value ?

Beyond this implementation protocol, it is important to consider the potential issues due to :

- the uncertainty margin on the value to be taken for V_{CE_ZTC}
- and the sensitivity of the new indicator to temperature variations

The figure 5 illustrates the impact of using an inaccurate V_{CE_ZCT} value on temperature sensitivity. When the used voltage $V_{CE\_ZTC}^{used}$ matches the true (or correct) characteristic voltage $V_{CE\_ZTC}^{thrue}$, the corresponding collector current I_{C_ZCT} remains nearly insensitive to temperature variations (central curve in the figure).

However, deviations from this ideal voltage introduce small temperature-dependent errors. The curves on either side of the central curve in Figure 5 demonstrate the extent of this error: when $V_{CE\_ZTC}^{used}$ deviates from $V_{CE\_ZTC}^{thrue}$, the

measured I_{C_ZCT} becomes slightly affected by temperature variations.

The method remains reliable as long as $V_{CE\_ZTC}^{used}$ falls within a range of around ± 3% of $V_{CE\_ZTC}^{thrue}$. Beyond this range, the accuracy of the aging indicator decreases, and temperature-induced variations become more significant, potentially impacting the precision of the diagnostic results.

As the method does not require very precise measurements, it is possible to use inexpensive sensors without significantly affecting reliability. This makes the overall implementation very inexpensive.

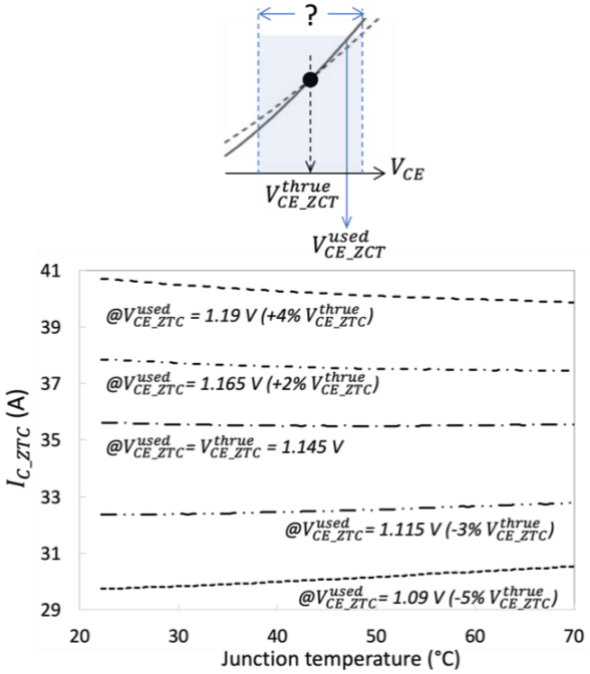

Fig.5 Measurements uncertainties

Full experimental demonstration

The demonstration has been made with an AC power cycling bench but it can be easily implemented on equipment operating in the field.

Test bench description

The test bench is illustrated in Figure 6, with a schematic of its principle shown in Figure 7. It consists of two completely independent parts: a load part and a test part (DUTs). The two parts are interconnected only through the load inductances and a shared DC bus. The bench supports testing up to three DUTs, with each DUT representing a leg (or phase), or a single DUT when testing all three phases together. Each DUT is connected to an inverter in the load section via a load inductance. Additionally, each inverter/DUT pair operates independently, forming a distinct test channel.

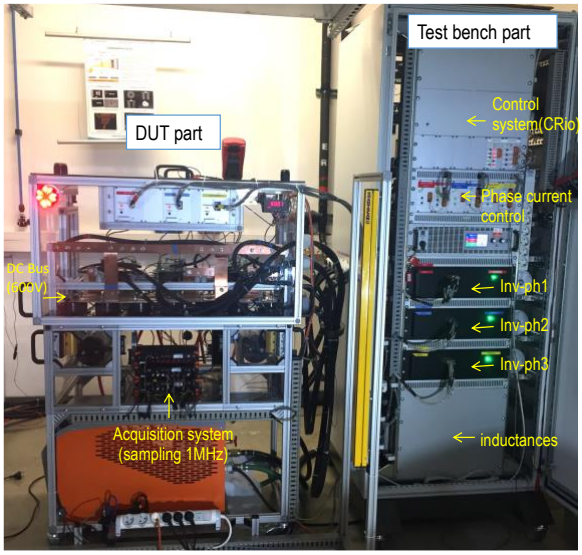

Fig.6: AC power cycling test bench.

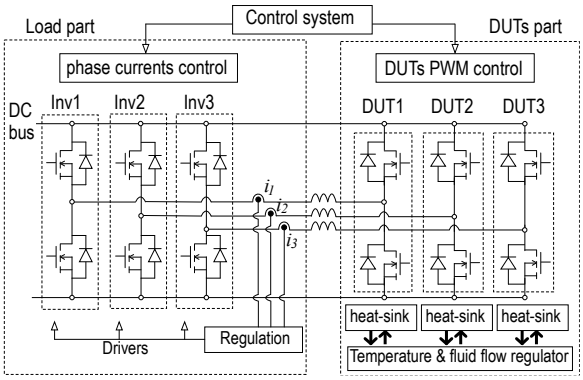

Fig.7: AC power cycling test bench schematic

The role of the load part is only to supply the desired current waveform to the DUTs through the load inductors. For this purpose, a control system is used to regulate the shape and level of the current in each channel. The test bench is capable to deliver:

- square current waveforms from few amps until ±500A,
- sinusoidal currents, until 500A peak current from DC to 500Hz,
- more complex currents as a combination of a square and sinusoidal waveforms,

Independently, in the "DUT part", the devices can be tested with any desired gate control strategy with switching frequency until 500 kHz (depending on the gate drivers) and with duty cycles from 1 to 99%.
The sequence instructions can be modified every millisecond allowing to change the type of cycle and current waveform at this frequency and to play very complex cycles. The two parts are controlled by a compactRio system from National

Instruments. The overall system is managed and monitored through a LabView interface. All parameters are monitored through the high-speed data acquisition system SIRIUS-HS from Dewesoft.

The devices used in the "test part" have a higher nominal power than the DUTs in order to greatly reduce their own stresses and that they remain reliable. The tested devices are cooled trough heat-sinks using a thermoregulator with a cooling fluid.

Test implementation and results

The method is tested here with a complex loading profile to demonstrate on-line state of health monitoring feasibility. Moreover, a power module that is even different from devices "A" and "B" presented above is used here, in order to confirm the validity of the previous observations. The tested IGBT power module is shown in fig.8, it is a 3-phase inverter from Infineon.

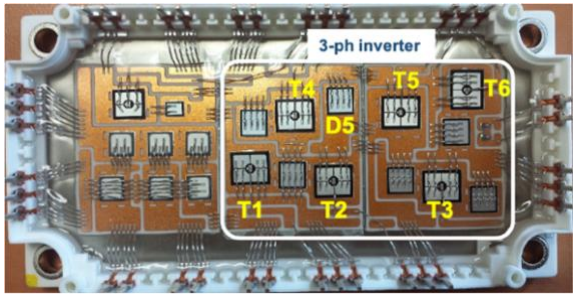

Fig. 8: Tested power module

The module was tested with a three-phase sinusoidal current with a phase shift of 120°. All the active chips (T1 to T6, fig.8) were monitored as well as the diode (D5). The generated power cycle is illustrated in fig.9 and consists of a total cycle of 26s, divided into 14s of heating and 12s of cooling. The heating period includes four distinct operating steps:

- Step 1 (1s) : Variable RMS current amplitude (ranging from 71A to 37A) and variable frequency (from 5Hz to 50Hz),
- Step 2 (1s) : Constant current amplitude (37A) and constant frequency (50Hz),
- Step 3 (1s) : Variable current amplitude (from 37A to 71A) and constant frequency (50Hz),
- Step 4 (11s) : Constant current amplitude (71A) and constant frequency (50Hz).

The temperature of the cooling fluid has been set to Tref = 38°C. Detailed views of the first and fourth steps are provided in figs.10 and 11.

The maximum (T_{jmax}) and minimum (T_{jmin}) junction temperatures are measured at the end of the heating and cooling periods, respectively (see fig.9). Additionally, to enable a comparison with the conventional aging indicator, the V_{CE} is measured at the end of each cooling period, when the junction temperature reaches T_{jmin}. These measurements are performed using short current pulses just before the start of the heating phase (see fig.10). During the power cycles, the measured T_{jmin} value was 35°C and the T_{jmax} was 105°C, so the temperature swing was ΔTj=70°C.

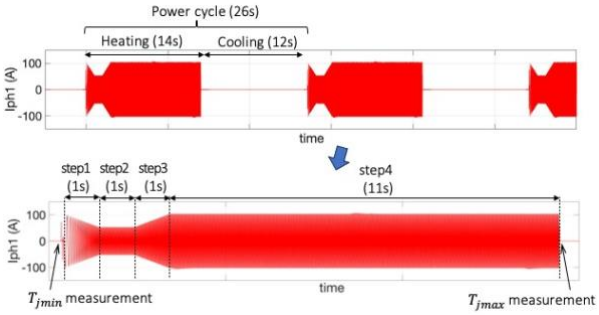

Fig.9: Load current cycles in one phase (top) and detailed view of the operating phases during the heating period (bottom).

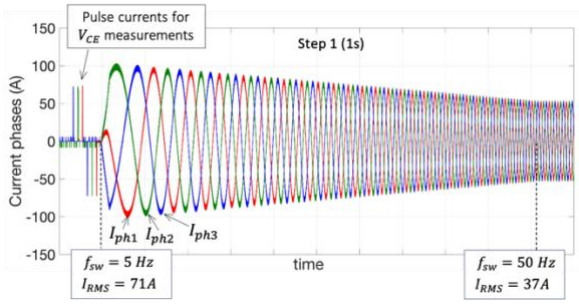

Fig.10: Current waveforms (all phases) during the step 1 of the heating period.

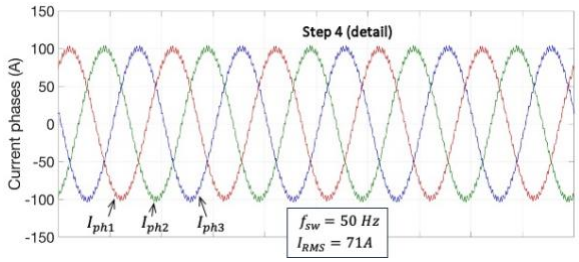

Fig.11: Current waveforms (all phases) during the step 4 of the heating period.

It is important to note that temperature and V_{CE} measurements using current pulses are required only for monitoring the traditional aging indicator for comparison purposes. These measurements are not necessary for the monitoring of the new

indicator (I_{C_ZTC}), which can be measured at any time during the heating period (i.e. during t_{ON}).

For the new indicator (I_{C_ZTC}), it was arbitrarily chosen, for demonstration purposes, to measure it once per sinusoidal cycle during the heating period and for each of the three current phases. As a result, approximately 700 measurements were recorded during each heating period (t_{ON}), corresponding to 700 sinusoidal cycles during this period. These measurements were taken while the junction temperature increased from T_{jmin} (35°C) to T_{jmax} (105°C), covering a wide range of temperatures. However, in practical operation, such a high number of measurements is unnecessary. A single measurement taken periodically may be sufficient for effective monitoring.

The I_{C_ZTC} measurement is performed during the current rise, precisely when the collector-emitter voltage V_{CE} crosses the reference value V_{CE_ZTC} (see fig.4).

As results, the aging led only to bond-wire contact degradations at the interconnection level, with no observable degradation in the solder layers. The evolutions of the new aging indicator (I_{C_ZTC}) are reported in fig.12 for the IGBTs chips and in fig.13 for the diode D5. Depending on the IGBT chips, the initial values of I_{C_ZTC} are approximately 16A (for T2 and T3) and 17A (for T1, T4, T5 and T6) due to characteristic dispersions. Concerning the diode D5, the initial value is significantly higher, at 55A.

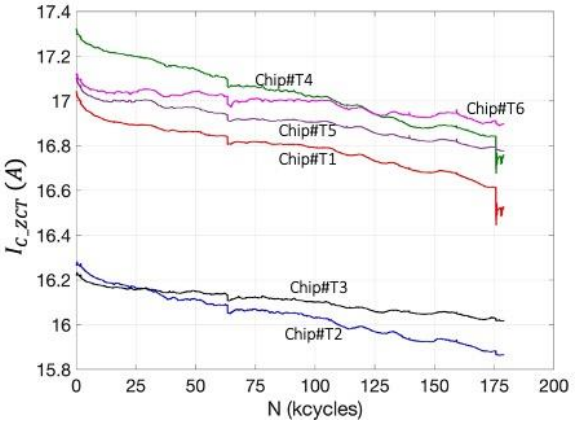

Fig.12: Evolution of the new aging indicator with cycles for the IGBT chips.

As expected, the aging indicator exhibits a general downward trend across all chips as the number of cycles increases. However, small fluctuations in values were observed, likely due to measurement inaccuracies, particularly in the interpolation process around the V_{CE_ZTC} reference value. Additionally, the small abrupt drops visible for T1 and T4 at 175 kcycles are attributed to bond wire lift-offs.

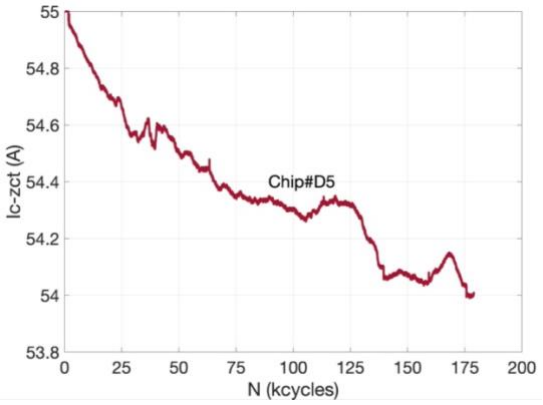

Fig.13: Evolution of the new aging indicator with cycles for the diode D5.

The relative variations of the new aging indicator (I_{C_ZTC}) for all chips (IGBTs and D5) are plotted in fig.14. These results can be compared to those of the traditional aging indicator (V_{CE}), shown in fig.15 for the IGBT chips only.

First, we can observe that both indicators correctly detect bond-wire contact degradations. The V_{CE} indicator with an increase in the forward voltage drop, and the I_{C_ZTC} indicator with a reduction in the current value at the ZTC crossover point. We can also observe that the T1, T2 and T4 chips degrade the fastest with one bondwire lift-off for T1 and T4 after 175 kcycles detected with both indicators. These 3 chips are located on the central substrate of the module (see fig.8) and are therefore thermally more stressed than the others.

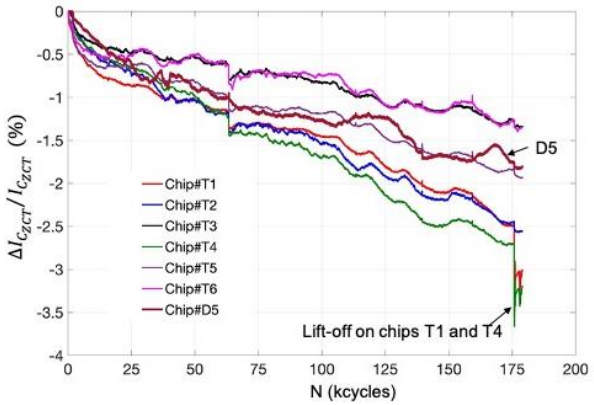

Fig.14: Evolution of the relative variations of the new aging indicator (I_{C_ZTC}) with cycles

The two aging indicators show a strong correlation, as shown in figure 16, where the relative variations of one indicator are plotted

against those of the other. However, we can observe that the I_{C_ZTC} indicator is twice as sensitive to contact degradations as the V_{CE}, making it a more effective diagnostic tool for detecting early signs of aging.

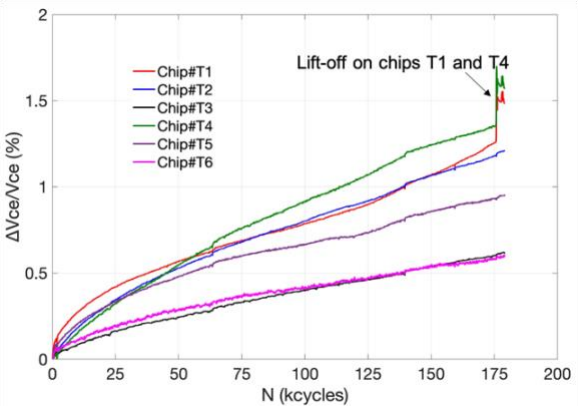

Fig.15: Evolution of the relative variations of the classical aging indicator (V_{CE}) with cycles.

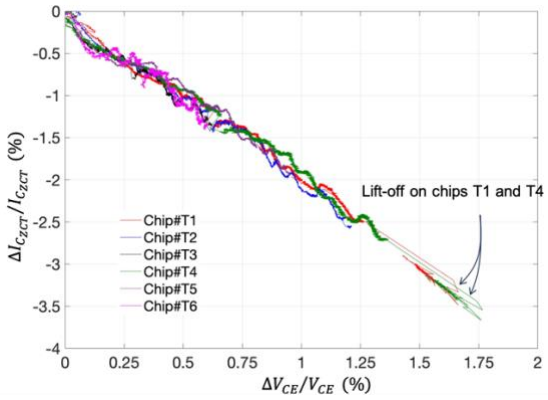

Fig.16: Correlation between the two aging indicators.

Conclusion

This paper introduces a novel temperature-independent aging indicator designed for on-line monitoring of bond wire degradation in IGBT power modules. Unlike traditional indicators, which rely on complex and costly temperature measurements impractical for field deployment, the proposed approach leverages the zero-temperature coefficient (ZTC) of the I-V characteristics. This enables a highly sensitive yet temperature-robust assessment of bond wire degradation. The implementation follows a straightforward two-step process:

- determining the ZTC point, which establishes a reference for monitoring;
- monitor the aging indicator during operation, enabling continuous health assessment.

Extensive experimental validation through power cycling tests demonstrates that the proposed indicator provides a strong correlation with conventional metrics, while offering enhanced sensitivity to early-stage degradation. This makes it a more effective tool for predictive maintenance of power modules.

Finally, this temperature-insensitive aging indicator represents a significant advance-ment in online condition monitoring for IGBT power modules. Its simplicity, cost-effectiveness, and superior degradation sensitivity position it as a promising solution for health diagnostics and predictive maintenance in power electronic systems.

References

[1]. S. Yang et al., “Condition monitoring for device reliability in power electronic converters: A review,” IEEE Trans. Power Electron., vol. 25, no. 11, 2010

[2]. H. Oh et al., “Physics-of-failure, condition monitoring, and prognostics of insulated gate bipolar transistor modules: a review,” IEEE Trans. Power Electron., vol. 30, no. 5, 2015.

[3]. S. Zhou et al., “Monitoring potential defects in an IGBT module based on dynamic changes of the gate current,” IEEE Trans. Power Electron., vol. 28, no. 3, 2013.

[4]. A. E. Ginart et al., “Online ringing characterization as a diagnostic technique for IGBTs in power drives,” IEEE Trans. Instrum. Meas., vol. 58, no. 7, 2009.

[5]. N. Degrenne, S. Mollov, "On-line Health Monitoring of Wire-Bonded IGBT Power Modules using On-State Voltage at Zero-Temperature-Coefficient", in Proc. of the PCIM Europe Conf., Nuremberg, 2018.

[6]. A. Singh, A. Anurag, S. Anand, “Evaluation of Vce at Inflection Point for Monitoring Bond Wire Degradation in Discrete Packaged IGBTs,” IEEE Trans. on Power Electronics, vol. 32, no. 4, 2017

[7]. G. Schlottig et al., "The limited usability of a ZTC-point in tracking IGBT degradation," CIPS, Berlin, 2022.

[8]. Z. Khatir, A. Ibrahim, R. Lallemand, " New temperature-independent aging indicator for power semiconductor devices – Application to IGBTs", Microelectronics reliability, Vol.164, January 2025, 115565.